

Resolution of seismic data acquired with vertical receiver arrays

John C. Bancroft, Yong Xu, and Carlos Rodriguez-Suarez

ABSTRACT

The resolution of vertical receiver array data may be evaluated by modelling the energy that illuminates a scatterpoint.

Scatterpoints below the receiver array receive illumination at all dips less than 45 degrees. Scatterpoints that are spatially removed from the receiver array will have limited illumination of dips. The construction of reflectors from the scatterpoints will also have a limited range of dips that can be imaged.

INTRODUCTION

Zero offset illumination of a scatterpoint

One model of seismic data considers all zero offset (or stacked) sections to be entirely composed of diffractions. These diffractions constructively interfere to form all reflections, and destructively interfere elsewhere.

Assume a scatterpoint to be semi-circular for 2-D poststack data, (or hemispherical for 3-D data). The normal reflections that define a diffraction, also define a corresponding continuum of reflection points on the scattering semi-circle. Therefore, in order to define a complete diffraction, all parts of the semi-circle need to be *illuminated* as illustrated in Figure 1. Any missing data on a diffraction will fail to illuminate part of the semi-circle, and will therefore fail to illuminate a reflector that is composed of organized scatterpoints.

The migration of the partially complete diffraction causes incomplete destructive interference around the scatterpoint, which causes a smear of energy or loss of resolution. In addition, any reflector that is composed of the scatterpoints, will also have dips that are not illuminated.

The partial illumination of a scatterpoint is illustrated in Figure 2, along with the resulting truncated diffraction. The energy missing from the diffraction causes a smear of the migrated scatterpoint. The dip of the smear is related to the missing dips of the diffraction.

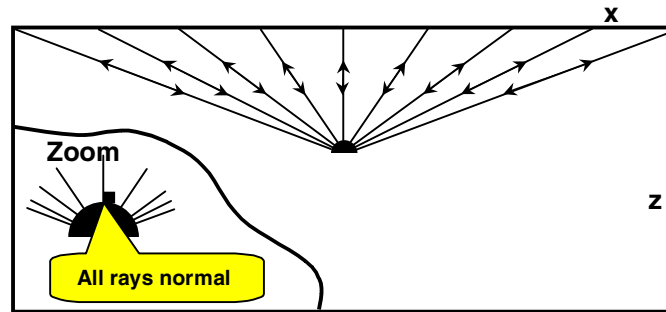
Processing that ensures all portions of the semicircle are equally illuminated, is often referred to as “true amplitude processing.”

Prestack illumination of scatterpoints with surface seismic

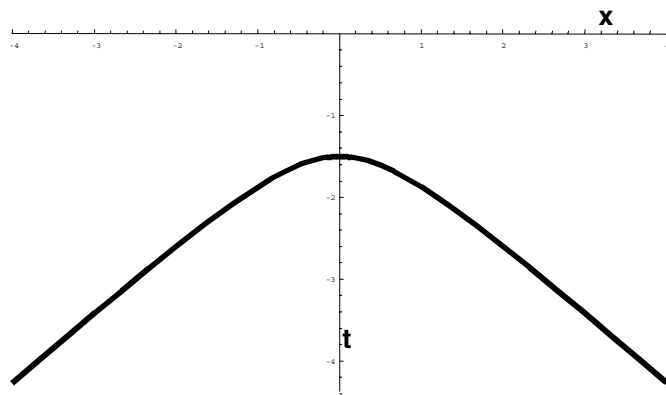
Consideration of prestack data enables the source and receiver to be separated, with angles of incidence and reflection that are non-zero to the reflecting plane. Each source/receiver raypath illuminates a point of the scatterpoint in an area where the

bisector of the incident and reflected ray is normal to the scatterpoint, as illustrated in Figure 3. This *bisector* will be used in the following sections to define the illumination of the scatterpoint, similar to the zero offset illumination.

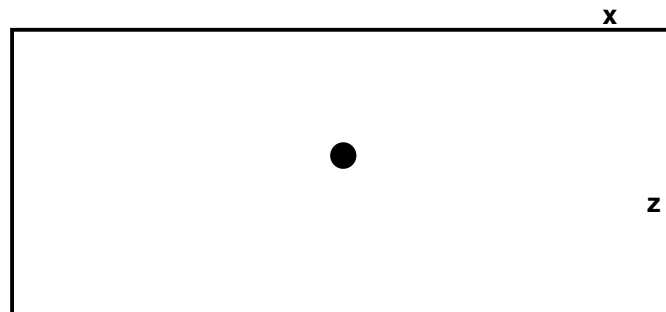
Only acoustic reflections will be considered with the assumption that the reflection coefficient remains independent of the angle of incidence.



a)



b)



c)

Figure 1. Illumination of a scatterpoint with a) showing the illuminating raypaths, b) the corresponding diffraction, and c) the migration. Optimum resolution of the scatterpoint can only be accomplished when the upper semi-circle of the scatterpoint is fully illuminated.

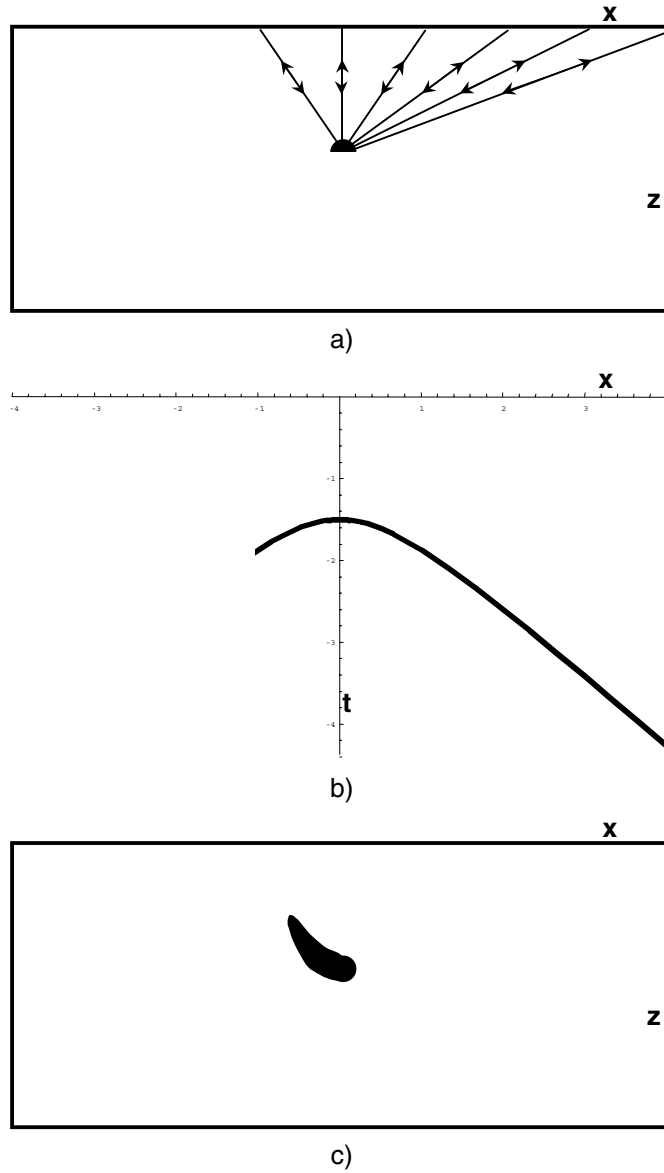


Figure 2. Partial illumination of a scatterpoint with: a) showing the illuminating raypaths; b) the corresponding diffraction; and c) the migration.

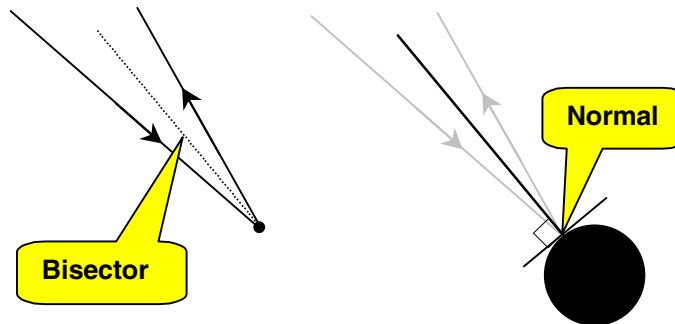


Figure 3. Offset raypaths illustrating the illumination area of the scatterpoint.

Figure 4 gives an example of five sources and receivers shooting into one scatterpoint. There will be a total of twenty-five raypaths that illuminate the scatterpoint. For this small offset and simple geometry, thirteen bisectors are unique and cover a reasonable area of the scatterpoint to dips of 45 degrees.

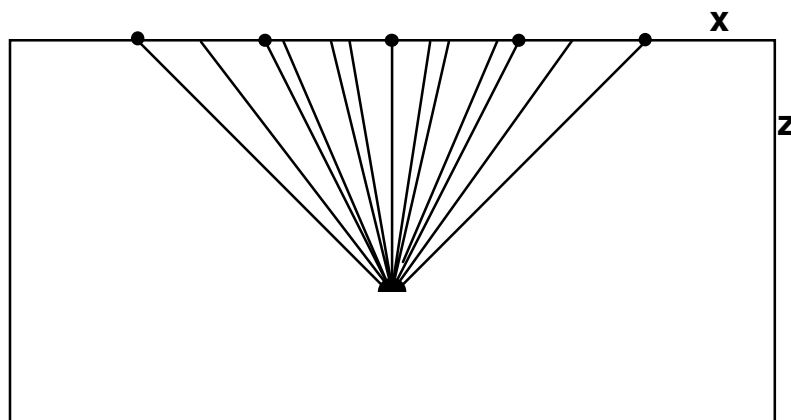


Figure 4. Bisectors for a scatterpoint with 5 sources shooting into 5 receivers located at the surface positions indicated by the dots.

VERTICAL ARRAY PROCESSING

Illumination of scatterpoints

A simple geometry of five surface sources and five vertically aligned receivers is shown in Figure 5. Part (a) of this figure shows the most counter-clockwise bisector while the most clockwise bisector is shown in (b). The total range of the bisectors, shown in (c), is surprisingly limited and is potentially a serious problem for vertical array projects. The limited range of bisectors that come from the vertical receiver array is illustrated in (d), which shows their range for one source and all receivers. The scatterpoint in Figure 5 is quite close to the receiver array, but fails to even have the horizontal portion illuminated.

The offset range of sources was limited in Figure 5 and could have contributed to the limited range of the bisectors. A continuum of surface sources that extend infinitely in each direction will now be evaluated in Figure 6. This figure also shows the location of a scatterpoint relative to the vertical array and the corresponding range of the bisectors. For simplicity, these labels will not be included in Figures 7 to 10. These figures show various locations of the scatterpoint (relative to the vertical array) and the range of the bisectors for various velocity distributions. The size of the vertical array (in gray) will indicate the relative depth of the scatterpoint. Each figure has been constructed with reasonable accuracy to establish ranges of the bisectors for scatterpoints in the proximity of a vertical receiver array.

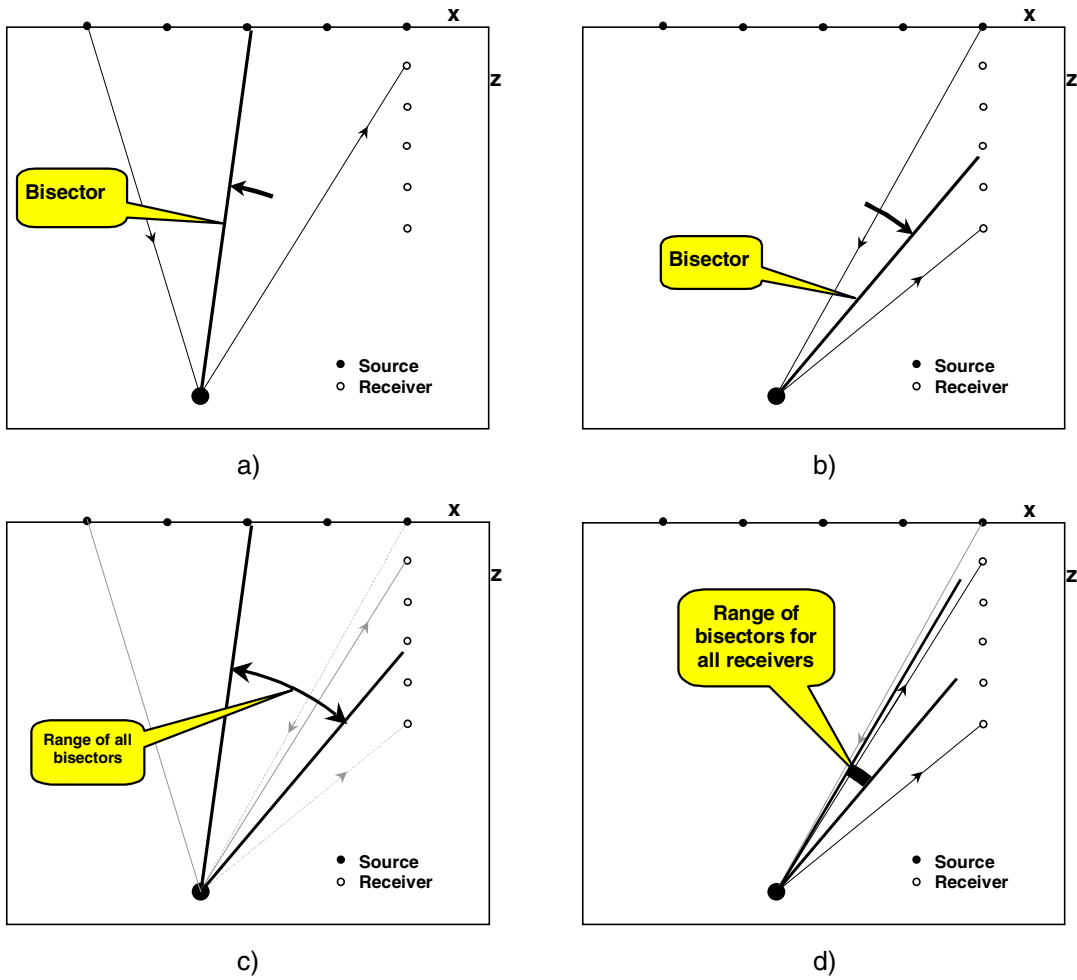


Figure 5. Bisectors for five surface sources and five vertical receivers: a) the most counter clockwise; b) the most clockwise; c) the range of bisectors for all source and receivers; and d) the range of bisectors for all receivers.

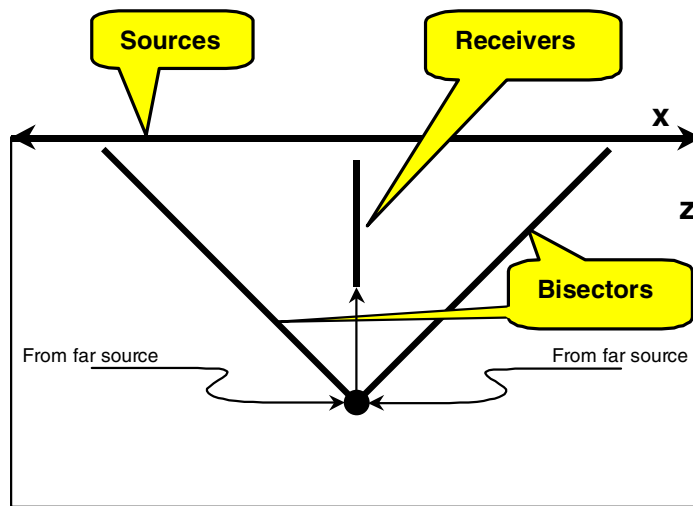


Figure 6. Example diagram that contains surface sources extending to infinity in each direction, a vertical receiver array, example rays from infinite offset sources and bisectors.

In Figures 7 to 9, the first four parts (a) to (d) consider a shallow scatterpoint (500m) that is slightly deeper than the receiver array (300m), while parts (e) to (h) considers a deeper scatterpoint (2000m) as illustrated by the length of the gray line that identifies the receiver array. In each figure parts (a) to (d) and (e) to (f) start with the scatterpoint immediately below the receiver array, and then increase in displacement to the left with a small, large, and then infinite displacement.

Figure 7 considers the constant velocity case with rays from far-offset sources arriving horizontally at the scatterpoint. These figures demonstrate that

- the range of bisectors remains insensitive to the depth of the scatterpoint relative to the depth of the deepest receiver
- an infinite offset array of sources will illuminate dips that slope towards the receiver array
- weakly illuminate horizontal dips, and
- only partially illuminate shallow dips that slope away from the receiver array.

Figure 8 considers velocities that increase linearly with depth i.e. $V = 3000(1 + Z)$. The rays follow circular paths as indicated. The infinite extent of the source offset is now limited to offsets that produce rays that only propagate in a downward direction, i.e. turning rays are excluded. Rays traveling to the receivers also curve and will be limited to directions that only decrease in depth (except for (c) to illustrate the problem). Now:

- the bisector range becomes limited to shallow depths and small offsets as the receiver rays can start in a downward direction, and
- moderate offset contains incident and reflected angles that approach 90 degrees.

Angles of incidence greater than 45 degree tend to have reduced amplitudes due to mode conversion. Consequently, Figure 9 contains the same linearly increasing velocity, but the angle of incidence is limited to 45 degrees. Part (c) shows that

- shallow scatterpoints, at moderate offsets, have a limited range of reflectivity, while
- (f) and (g) indicate that the offsets of deeper scatterpoints should be less than their depth, and
- large source offsets may not be required.

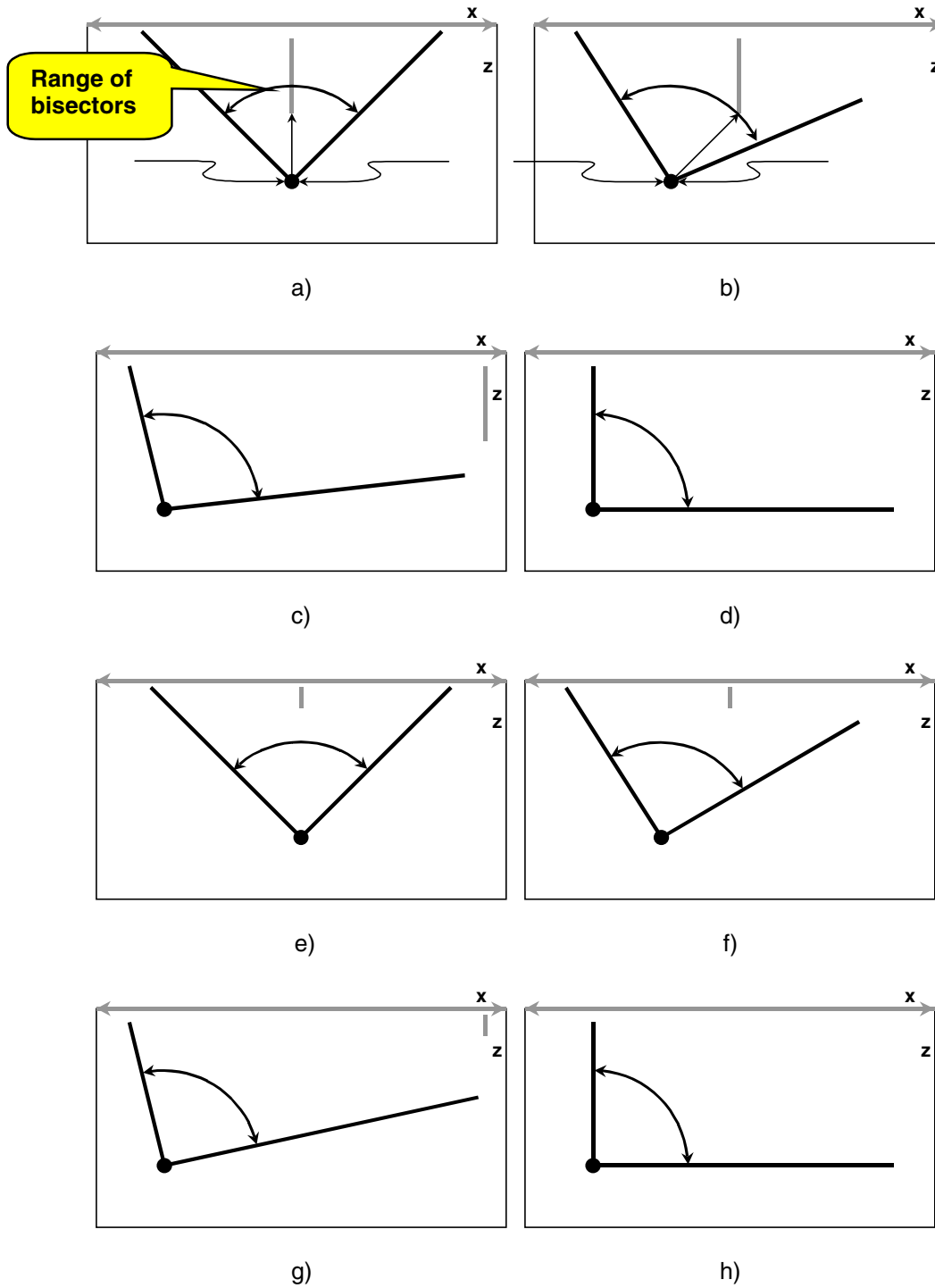


Figure 7 Constant velocity. Simplified example of the range of bisectors for positions of the scatterpoint relative to the vertical array: a) shallow and below the vertical array (VA); b) shallow and slightly displaced from the VA; c) shallow and well displaced; d) shallow and infinitely displaced; e) deep relative to, and below the VA; f), deep and slightly displaced; g) deep and well displaced; and h) deep and infinitely displaced.

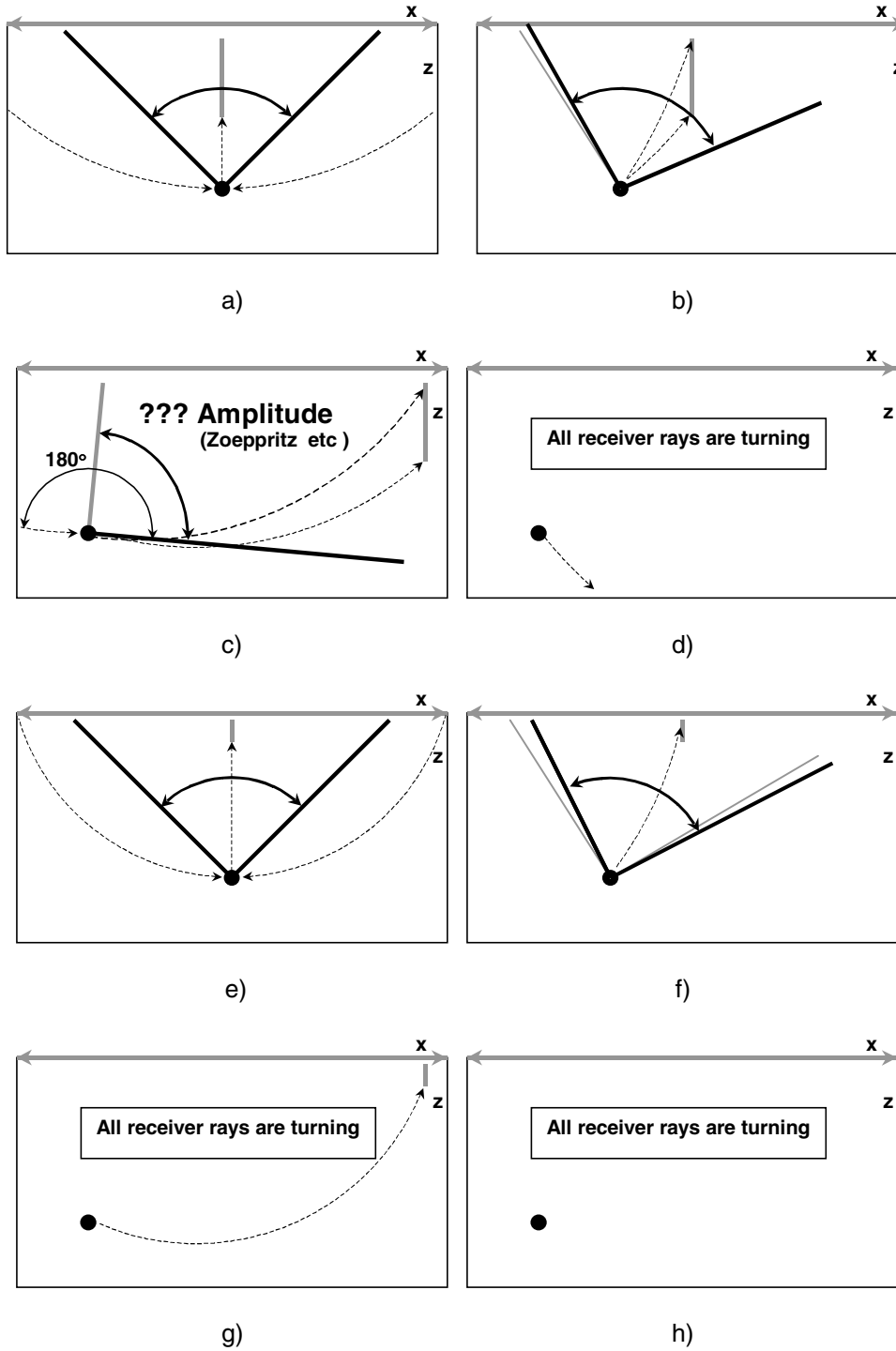


Figure 8. Linear $V(z)$, $V = 3000(1 + z)$. Simplified example of the range of bisectors for positions of the scatterpoint relative to the vertical array: a) shallow and below the VA; b) shallow and slightly displaced from the VA; c) shallow and well displaced; d) shallow and infinitely displaced; e) deep relative to, and below the VA; f), deep and slightly displaced; g) deep and well displaced; and h) deep and infinitely displaced.

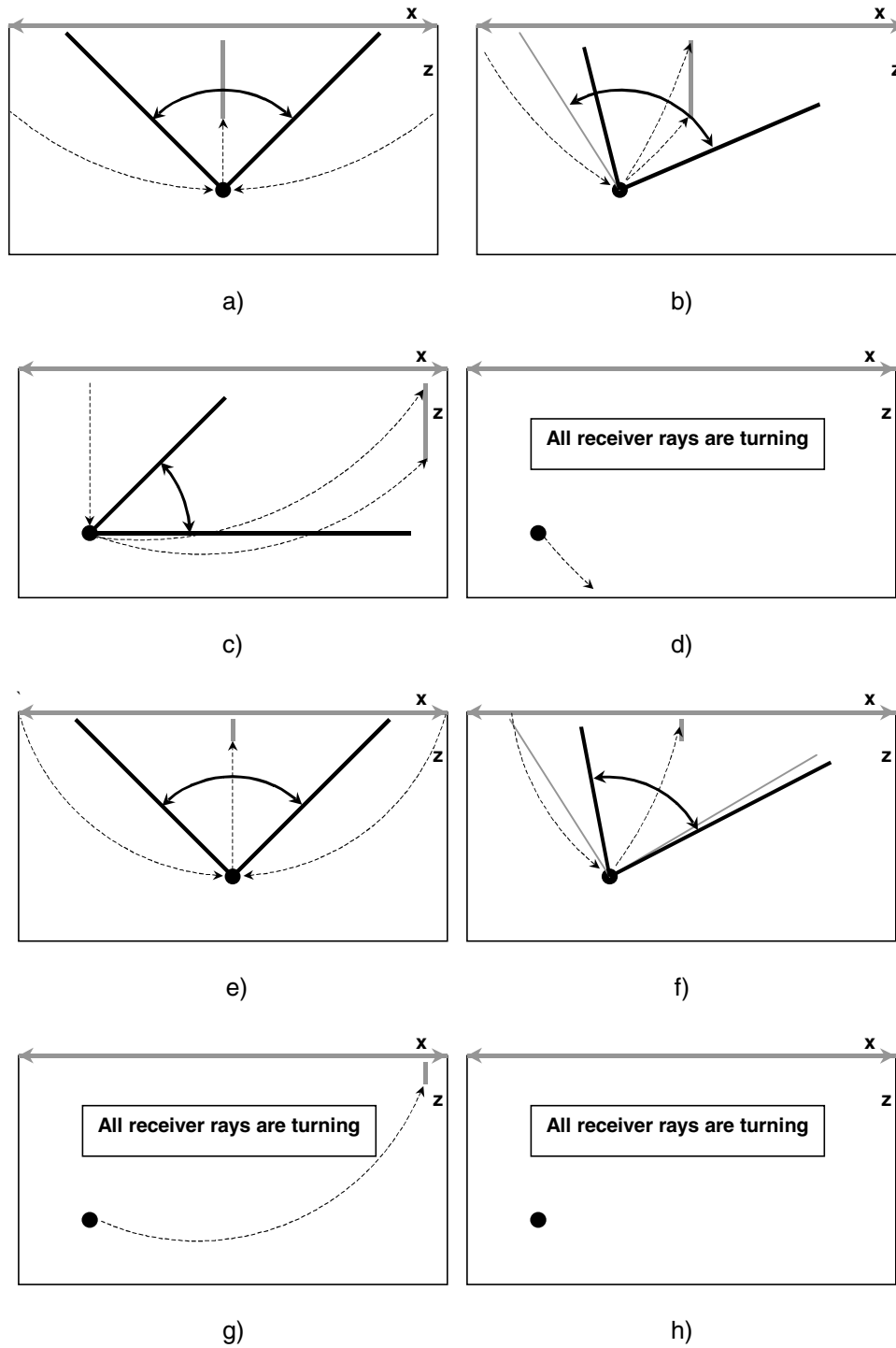


Figure 9 Angle of incidence limit to 45 degrees and linear $V(z)$. Simplified example of the range of bisectors for positions of the scatterpoint relative to the vertical array: a) shallow and below the VA; b) shallow and slightly displaced from the VA; c) shallow and well displaced; d) shallow and infinitely displaced; e) deep relative to, and below the VA; f), deep and slightly displaced; g) deep and well displaced; and h) deep and infinitely displaced.

Figure 10 also limits the angle of incidence to 45 degrees, but has a linearly decreasing velocity with depth. This model, however, is flawed in that the velocity

soon becomes zero and does not represent a reasonable geology. It does, however, illustrate that the curved rays now tend to aid in imaging with the vertical receiver arrays by increasing the separation of the raypaths as they travel to the receivers. Geological applications may apply to ground penetrating radar or in areas below basalt or carbonate layers.

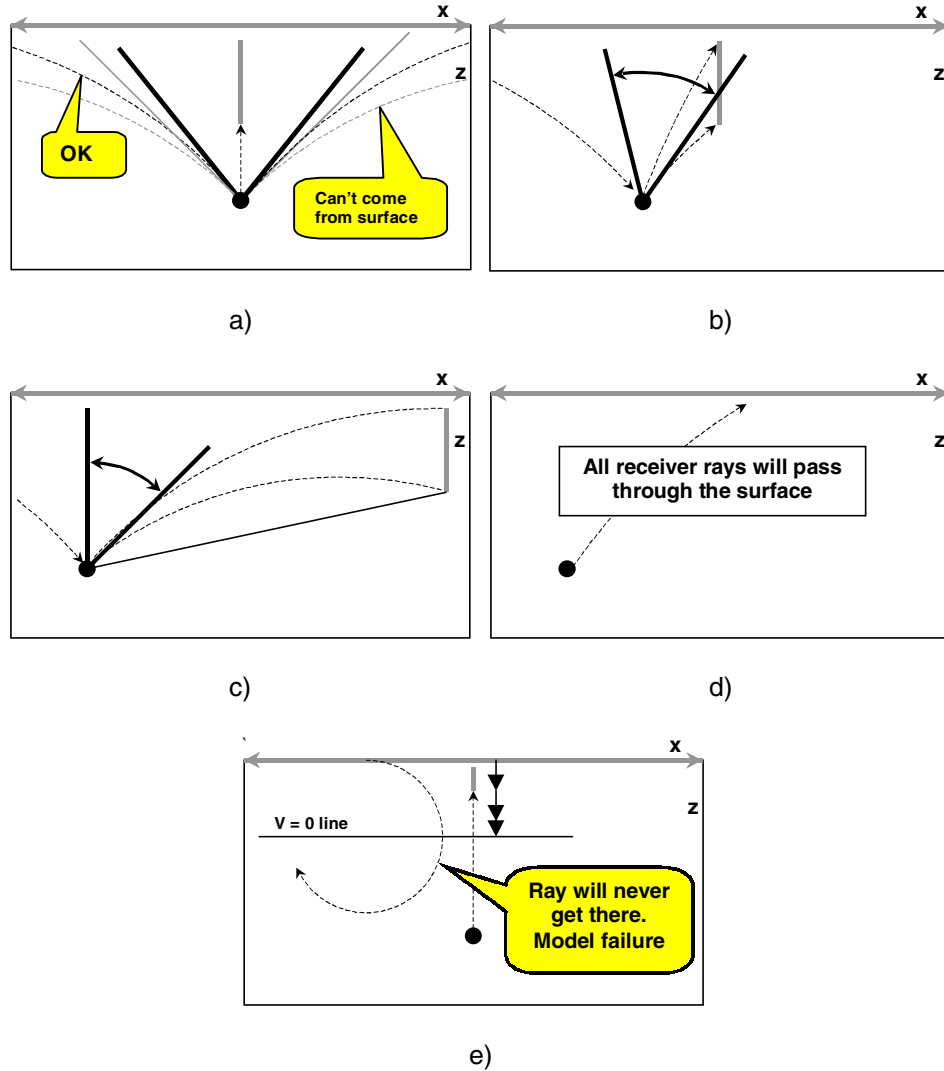


Figure 10. Angle of incidence limited to 45 degrees and linear $V(z)$. Simplified example of the range of bisectors for positions of the scatterpoint relative to the vertical array, a) shallow and below the VA, b) shallow and slightly displaced from the VA, c) shallow and well displaced, d) shallow and infinitely displaced, and e) deep relative to, and below the VA.

The above figures are limited to simple geometry but do indicate potential problems with the vertical array method. These limitations imply that 3-D acquisition projects that utilize vertical cables should have many of them closely spaced with horizontal dimensions that match the depth of the seismic targets. The offset range of the sources may also be reduced, indicating that the vertical cables could be moved more often in a roll-along method similar to land acquisition.

It was also interesting to note that the kinematics of the imaging appears to be independent of the number of receivers and the length of the receiver array. However, other factors such as multiple attenuation and improvement in the signal to noise ratio (SNR) will depend on the number and length of the receiver array.

THE BISECTOR AND THE PRESTACK MIGRATION ELLIPSE

For constant velocities, the bisector is easily defined on the prestack migration ellipse using DMO and poststack migration as illustrated in Figure 11. DMO moves one sample of input energy to many positions that may be considered to be at zero offset. Each of these samples may be poststack migrated with semi-circles that become tangent to the prestack migration ellipse. The point of tangency between the circle and the ellipse has a normal that passes through the center of the migration semi-circle. This normal defines the bisector.

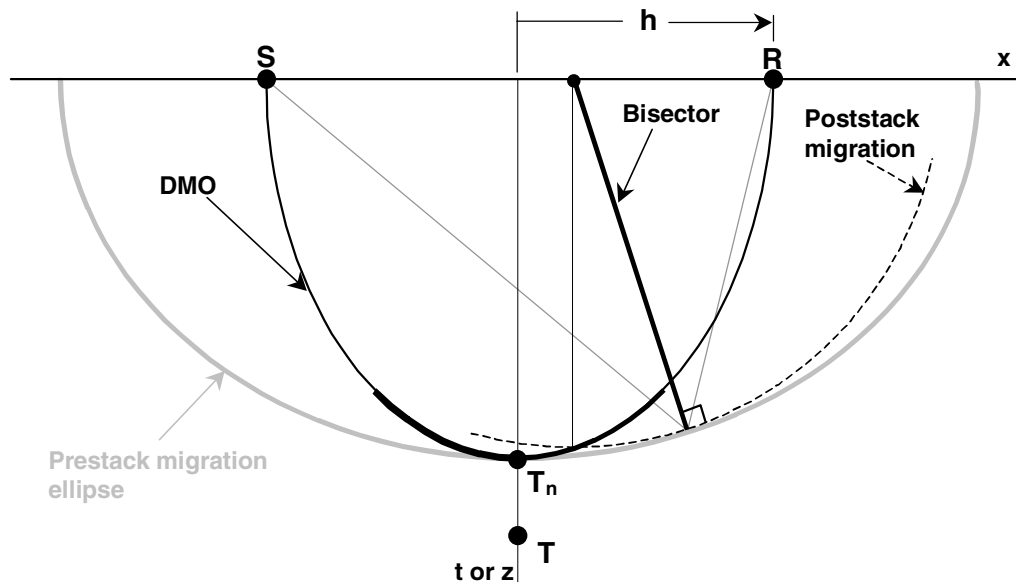


Figure 11 The location of the bisector may be defined using the DMO ellipse, the poststack migration semi-circle, and the prestack migration ellipse.

THE BISECTOR AND THE EQUIVALENT OFFSET

The bisector represents the normal to the reflector, (or scatterpoint), and represents the true zero offset raypath. In contrast, the equivalent offset defines a colocated source and receiver position on the surface that maintains the same total traveltimes of the offset raypath. For small dips, the equivalent offset raypath has a similar angle to the bisector and may be used to help define the range of dips that illuminate a scatterpoint. Consequently, a scatterpoint hyperbola on a CSP gather may aid in establishing the illumination of a scatterpoint, especially if the energy on the scatterpoint hyperbolas is limited.

EXAMPLES USING NUMERICAL MODELLING

A MATLAB program produced two sets of model data for evaluating the resolution that can be obtained with one vertical receiver array. Both models had twenty receivers extending from a depth of 20m to 400m and four scatterpoints located at depths of 500m, 1000m, 1500m, and 2000m below the receiver array.

The first model contained 441 sources on a 2000m by 2000m grid with 100m spacing, and with the receiver array located at the center (1000m, 1000m). Four additional scatterpoints were placed at the same depth of those above, but at an offset of 500m to the left of the receiver array.

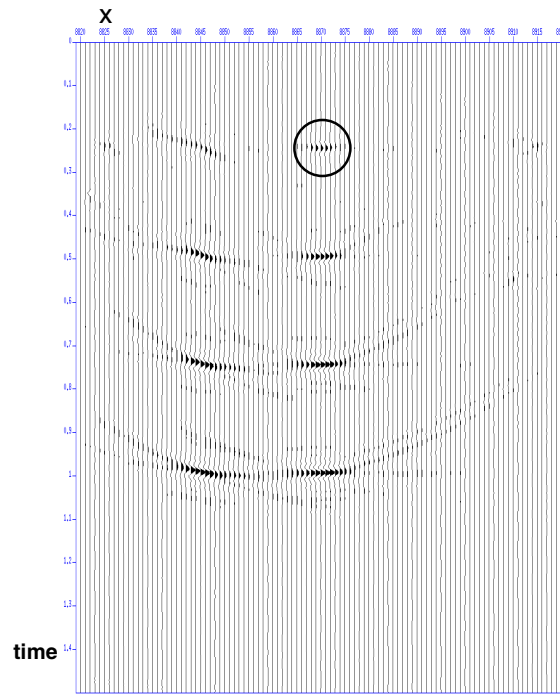
The second model contained 1681 sources on a 4000m by 4000m grid with 100m spacing and the receiver array located at the center (2000m, 2000m). Eight additional scatterpoints were placed at the same depth of those above, but at an offset of 1000m to the left and right of the receiver array.

The source record contained all possible offsets with a recording time of 2.0 seconds.

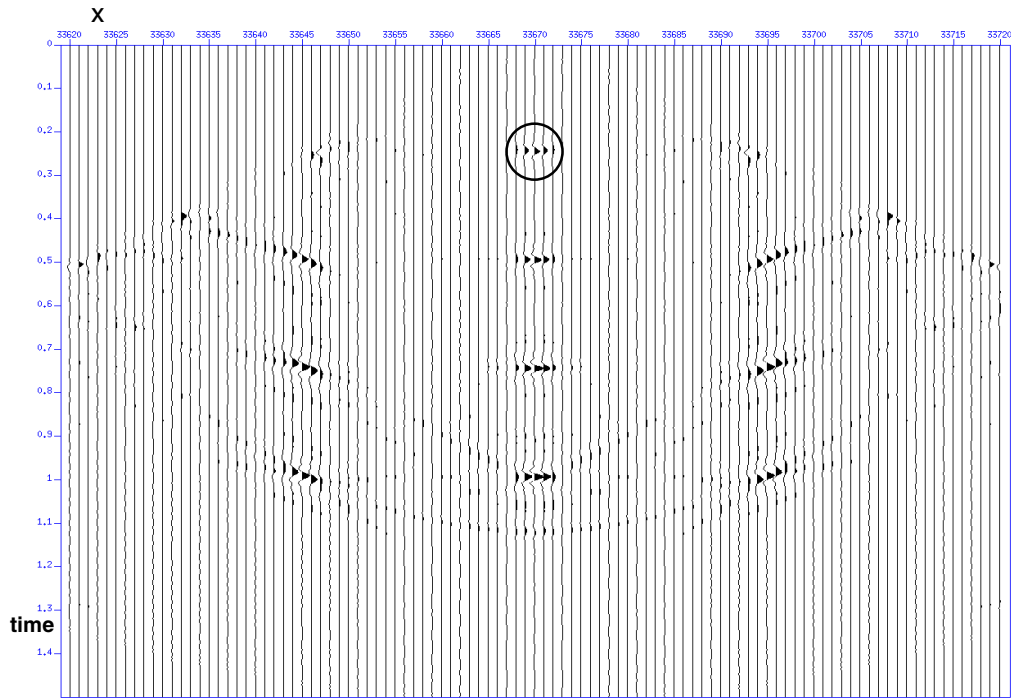
The source records were processed with a Seismic Unix (SU) equivalent offset migration (EOM) algorithm to CSP gathers on a 2-D line that passed through the all scatterpoint and the receiver array. The gathers were Kirchhoff NMO corrected to produce two stacks. The first model created migrated traces at 20m interval and the second at 40m intervals.

The zero-offset recording time of the scatterpoints occur at 250, 500, 750, and 1000 ms as illustrated in Figure 14, which contains the prestack time migrated sections of both models. The plots are scaled to represent equal vertical and horizontal distances. Figure 14a contains model 1 with an additional set of receivers 500m to the left of the array and Figure 14b contains model 2 in which additional scatterpoint are located 1000m to the left and right of the array. The (a) scatterpoints below the receiver array decrease in resolution with depth while those in (b) remain relatively constant as referenced by the identical circles. The increased source offsets of model 2 provide more offset information in (b), there by increasing the resolution. This difference in offset energy can be observed in the CSP gathers of Figure 15.

The loss of resolution in the offset scatterpoint is also apparent in Figure 14. Note the imaged scatterpoints contain a tilt that is due to the asymmetrical 3-D illumination, which is illustrated in the CSP gathers of Figure 16. The loss of the inside trace information is due to the limited range of bisectors from all azimuths. Only the steeper dips that face the receiver array are illuminated. This loss of illumination is more accurately manifest by the inability of the neighbouring traces to cancel the scattered energy.

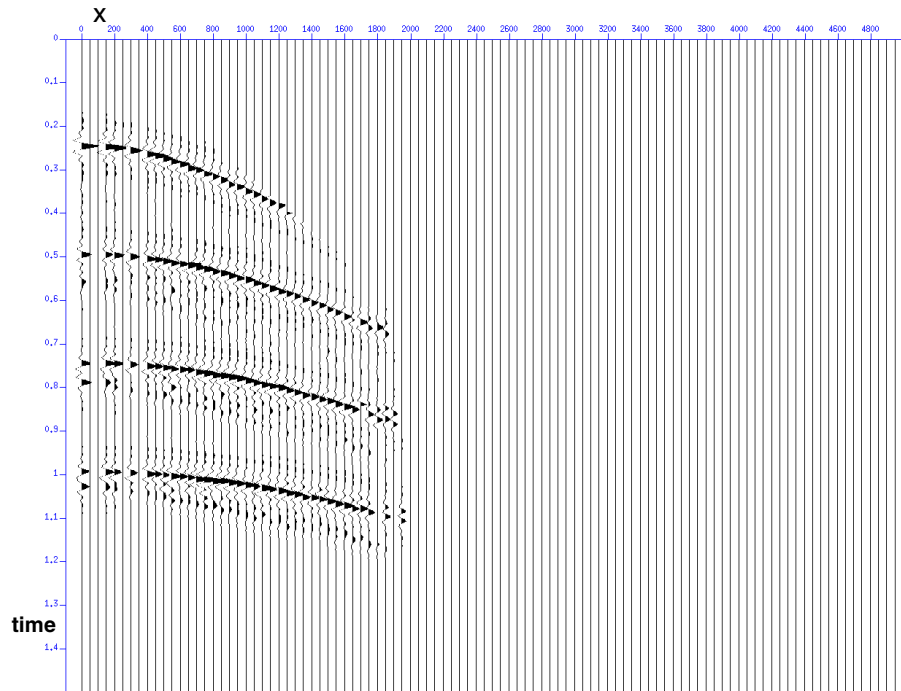


a)

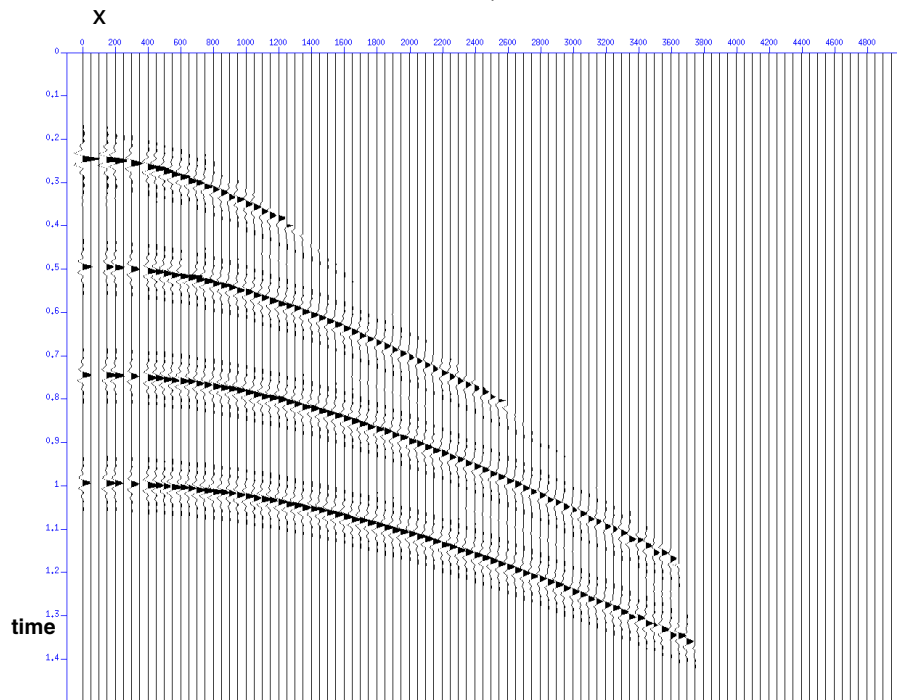


b)

Figure 14 Prestack migrated sections of a) model1 with a 2000m by 2000m grid of sources, and b) model 2 with a 4000m by 4000 grid of sources.

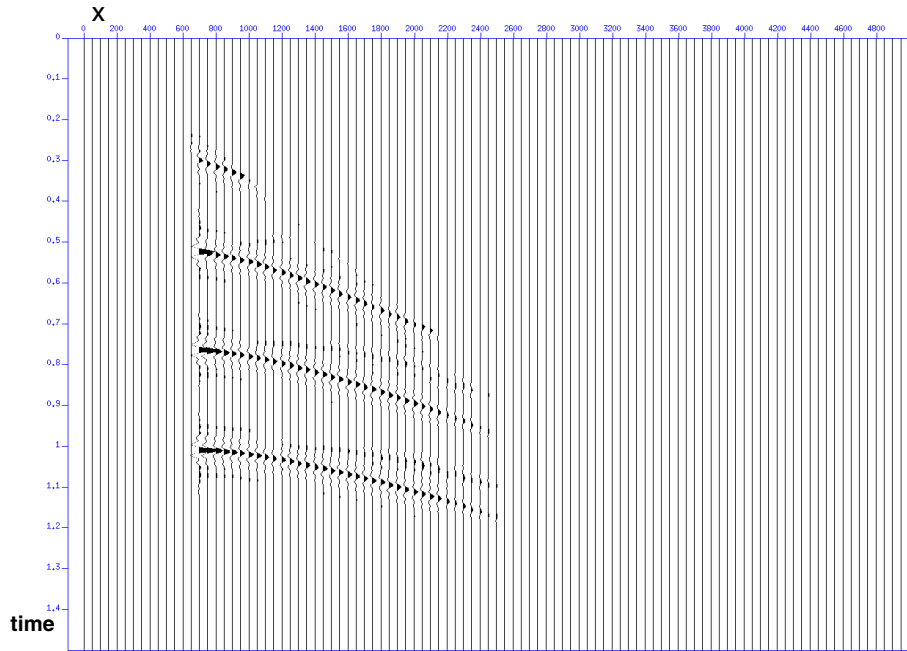


a)

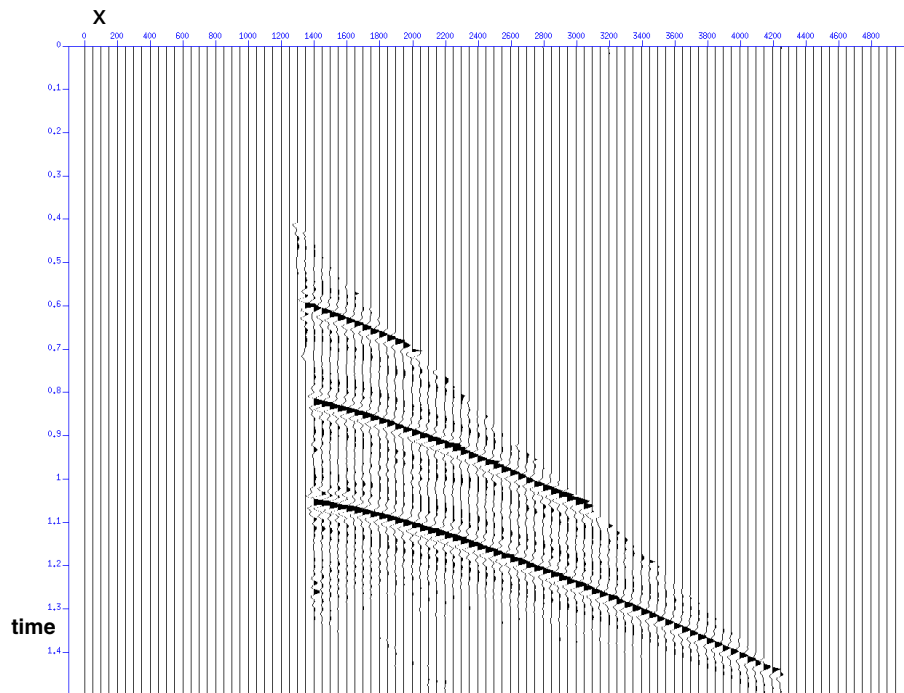


b)

Figure 15 CSP gather for the scatterpoint below the receiver array for a) model 1, and b) model 2 in which the offset energy is greater.



a)



b)

Figure 16 CSP gathers for a) located at the 500m offset scatterpoints in model 1, and b) for the 1000m offset scatterpoints of model 2. Note the loss of small offset information.

CONCLUSIONS

The use of the bisector between the incident and reflected rays is useful in defining the illumination and therefore the resolution of scatterpoints that surround a vertical receiver array.

Acquisition projects that used vertical receiver arrays may have difficulty illuminating all the dips of a neighbouring scatterpoint. The resulting reflectors will also have dips that will only be illuminated if they are dipping toward the receiver array. Consequently, in order to illuminate a structured surface, the receiver arrays will require a separation that is less than the depth of interest.

The length and number of receivers in the vertical array appear to have little effect on the illumination of surrounding reflectors.

The curved rays in areas with vertically increasing velocity (in depth) may further limit the illumination around a vertical receiver array. However, areas with decreasing velocity (with depth) may find a slight improvement in the areas of illumination.

Numerical modelling projects illustrate the loss of resolution on scatterpoint in the neighbourhood of a single vertical receiver array.

REFERENCES

Bancroft, J. C., Geiger, H. D., and Margrave, G. F., 1998, The equivalent offset method of prestack time migration: *Geophysics*, Vol.63, No. 6, p. 2042-2053.